A simple three-dimensional vortex micromixer

Maureen Long,[1] Michael A. Sprague,[2] Anthony A. Grimes,[1] Brent D. Rich,[1] and Michelle Khine[1,a)]

[1]*School of Engineering, University of California, Merced, Merced, California 95344, USA*
[2]*School of Natural Sciences, University of California, Merced, Merced, California 95344, USA*

We demonstrate rapid homogenous micromixing at low Reynolds numbers in an easily fabricated and geometrically simple three-dimensional polystyrene vortex micromixer. Micromixing is critically important for miniaturized analysis systems. However, rapid and effective mixing at these small scales remains a persistent challenge. We compare our micromixer's performance against a two-dimensional square-wave design by examining its effectiveness in mixing solutions of dissimilar concentration as well as suspension solutions comprised of microparticles. Numerical simulations confirm our experimental observations and provide insights on the self-rotational mixing dynamics achieved with our simple geometry at low Reynolds numbers. This rapid, robust, and easily fabricated micromixer is amenable readily to large scale integration. © *2009 American Institute of Physics*. [DOI: 10.1063/1.3089816]

The ability to effectively mix dissimilar fluids is fundamentally important in biological and chemical processing and analysis. Mixing macromolecular solutions at the microscale is necessary for biochemical reactions, chemical synthesis, and biological processes.[1–3] Moreover, rapid mixing is critical, for example, in biochemical detection involving hybridization analyses, immunoassays, and cell-molecule interactions.[4,5] Despite its importance to miniaturized "laboratory on a chip" analysis systems, micromixing is ironically difficult to achieve within such microscale systems.[6–9] Because molecular diffusion dominates mixing at these small scales with persistent laminar flow [the transition to turbulent flow occurs at Reynolds (Re) numbers greater than 2000 in straight microchannels[9]], large molecules with low diffusion coefficients in particular require considerable time to mix.[10] For effective mixing, interfacial surface areas must therefore be maintained. While this can be achieved by flowing the dissimilar solutions in tangent over considerable lengths, long microfluidic channels (on the order of centimeters) negate the intended benefits of miniaturization.[11] More critically, rapid mixing remains a challenge.

Therefore, to achieve rapid and effective mixing in microscale systems, more elaborate strategies have been adopted. Active mixers and/or complex passive mixers are typically required. Active mixers actuate by moving parts or through externally applied forces (e.g., pressure or electric fields). For example, Oddy *et al.*[10] used oscillating electric fields to create electro-osmotic flow that induces electrokinetic instability to stir microflow streams. Hellman *et al.*[12] used highly focused nanosecond laser pulses to create cavitation bubbles that expand and then collapse to disrupt the laminar flow of parallel fluid streams in microfluidic channels, producing a localized region of mixed fluid. Niu *et al.*[13] developed a chaotic micromixer based on hydrodynamic pulsating pumps to disturb the liquid. Other strategies for active mixing include magnetic stirring and ultrasound.[14,15] Rotary micromixers require very high rotational speeds and Re numbers in the hundreds to achieve turbulent mixing.[9] Moreover, these active mixers typically require a more complex

setup (laser, voltage, or other actuating source) and subject potentially fragile specimens (e.g., cells or cellular components) to considerable external energy.

Passive mixers utilize system geometry to create favorable hydrodynamics and avoid many of the complications associated with active mixers. A two-dimensional (2D) planar "square-wave" mixer sustains two fluid streams tangentially to achieve mixing by molecular diffusion over considerable lengths.[16] Alternatively, chaotic-mixing strategies leverage transverse flows that expand the interfacial area between solutions by folding and stretching.[17] Sudarsan and Ugaz[11] developed an innovative approach that leverages naturally arising transverse (Dean) flow fields using a planar split-and-recombine and an asymmetric serpentine micromixer configuration. Stroock *et al.*[18] created chaotic mixing by using relief structures on the floor of the microfluidic channel.

While rapid mixing in 2D is considerably more difficult and requires such geometrically ingenious strategies, up to now, three-dimensional (3D) out-of-plane mixing has been limited due to the challenges associated with microfabricating such devices, which could require up to days.[10] Liu *et al.*[16] used eddies generated at the bends of a helical microchannel for chaotic advective mixing. Lin *et al.*[19] developed a complex three-layer glass self-rotational vortex mixer for low Re in which two inlet channels divide into eight individual channels tangent to a 3D circular chamber.

With device dimensions similar to those of other studies,[19] we are able to homogeneously and rapidly mix using a geometrically simple and easily fabricated design. As shown in Fig. 1, the device employs one inlet channel, one vertical drop, and one outlet channel where the inlet and outlet channels (hydraulic diameters of 0.27 and 0.40 mm, respectively) are tangentially aligned to the cylinder of diameter 1.50 mm and vertical height of 1.55 mm. We presented previously an approach for the ultrarapid direct patterning of complex 3D polystyrene microfluidic chips.[20] Here we demonstrate the utility of such a 3D chip by comparing its mixing enhancements over a 2D square-wave mixer. Because this approach requires no photolithography and has minimal chip "footprint" area, our 3D micromixer is amenable to

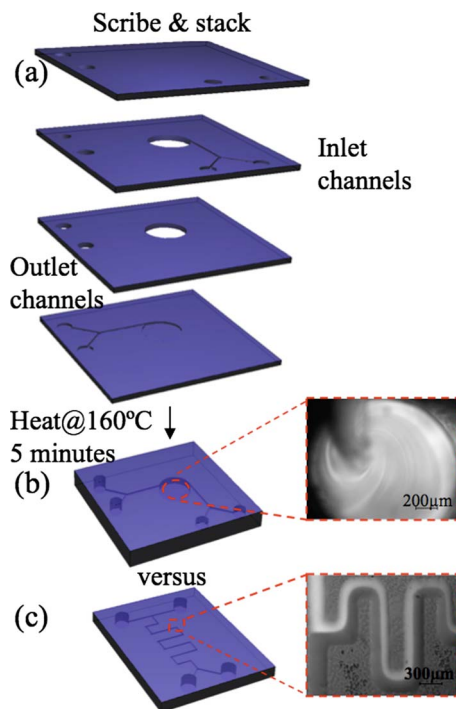a)Electronic mail: mkhine@ucmerced.edu.

FIG. 1. (Color online) Schematic of (a) fabrication process and (b) final 3D vortex micromixer (note that the inlet and outlet channels are on different planes) vs the (c) 2D square-wave. Insets of fluorescence-overlaid bright-field images illustrate the mixing dynamics of each approach.
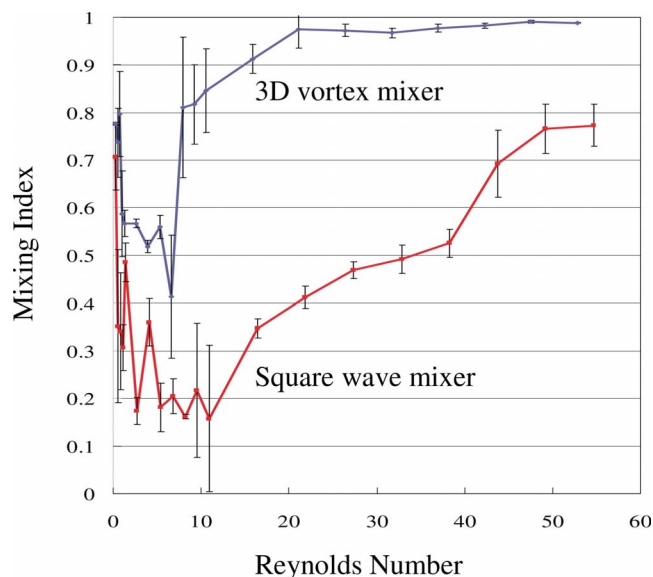

FIG. 2. (Color online) Mixing index as a function of Re number for both the 3D vortex and 2D square-wave micromixers. Error bars represent standard error of the mean.

large-scale integration in which these mixers can be arrayed readily in parallel.

We mechanically etch the pattern designs on the children's toy Shrinky Dinks, which are biaxially prestressed polystyrene sheets.[21] After heating,the engraved microchannels shrink in plane by approximately 60% and increase in height by over 700%. A more detailed description of the fabrication is described elsewhere.[20]

To compare mixing effectiveness, we test both 2D square-wave and 3D vortex mixers (Fig. 2). For each mixer, we simultaneously flow water diluted with two different concentrations of blue dye (McCormick Dye, Inc.) using a syringe pump (KD Scientific). We used volumetric-flow rates (Q) (vortex range: 5–1000 μl/min; square-wave range: 0.83–166.5 μl/min) that correspond to Re number range of 0.3–55.0, where Re=Q/D ν; D is the hydraulic diameter (calculated as $4 \times$area/perimeter) of the inlet channel and ν is the kinematic viscosity, taken here as 1.156×10^{-6} m^2/s. The hydraulic diameter of the square-wave channel is 0.04 mm; the device has 6 periods, each with a length of 7.22 mm and width of 2.04 mm such that the two dissimilar fluids are in contact for a total 44.95 mm. Note that for these PDMS (polydimethylsiloxane) devices, the cross sections of the channels are rounded as described elsewhere.[21] We collected each mixed solution in their respective branched outlet channel. We then quantified the absorption optical density of the solutions with a photometric microplate absorbance reader (Multiskan EX, Thermo Electron). We define the mixing index to be one minus the difference in intensity of the outlets divided by the difference in intensity of the inlets. A value of zero would indicate the poorest mixing and a value of one as the best.

Enhanced mixing is found using the vortex mixer; its mixing index is better than the square wave channel for all Re numbers tested (Fig. 2). Our mixing index for the square-

wave mixer is in good agreement with previous reports.[16] We also found that compared to mixing-index fluctuations in the square-wave mixer, the mixing index of the 3D vortex micromixer is more stable at different flow rates. Notably, the "good" mixing in both designs at extremely low Re is because we allowed the mixing to take as much time as necessary for a given flow rate and only measured the constant volume that we collected from the chip.

To ensure that the improved mixing is indeed due to the vertical drop and not due solely to the cylindrical expansion and constriction of the channel, we also tested a similar geometry but in two dimensions. Specifically, the 3D vortex geometry, minus the vertical drop, was molded out of PDMS. This "2D vortex micromixer" has an inlet, cylindrical chamber, and outlet all in the same plane. The inlet hydraulic diameter is 0.04 mm, and the chamber diameter is 1.95 mm; the system height is approximately 0.05 mm as it was made in the same replication molding fashion as the square-wave mixer. We performed the same mixing experiment. Even at Re numbers greater than 40 (which corresponds to mixing indices of over 0.95 for the 3D geometry), the mixing-index range for the 2D device reaches a maximum value of less than 0.50 (data not shown). From this, we conclude that the effects of traversing out of plane influence mixing.

To understand better the mechanisms of mixing in the 3D chamber, we employed a spectral finite-element model of the unsteady incompressible Navier–Stokes equations; the program is described in detail elsewhere.[22] The 3D model consisted of 960 unstructured hexahedron elements, where each element had eighth-order basis functions. The inlet, outlet, and chamber hydraulic diameters match those of the 3D vortex mixer used in our experiment; parabolic inlet and outlet velocity profiles were assumed.

Figure 3 shows top and side views of the chamber with streamlines for 25 particles released at the inlet for Re=5.2, 10.6, and 26.4. Re=5.2 is near the value corresponding to the lowest mixing index seen in the experiments (Fig. 2) for the3D mixer. Accordingly, the streamlines show very little vortex motion. The streamlines for Re=10.6 show increasingvortex motion; these streamlines are representative of the flow in the range of 6.6<Re<21.0, where the number of
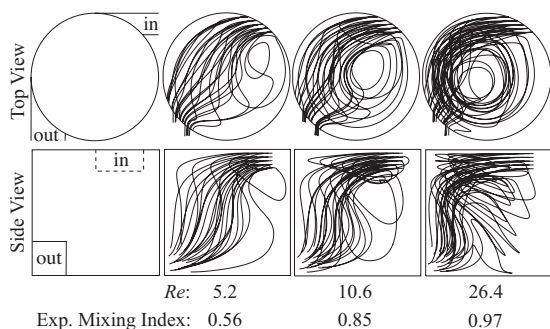
FIG. 3. Streamlines for 25 particles released at the inlet for various Re numbers calculated with the computational model. Also listed are corresponding experimentally determined mixing-index values.

streamlines exhibiting vortical motion increases with increasing Re. This agrees with experiments (Fig. 2), which show a monotonic increase in mixing index in this range of Re numbers, reaching near-optimal mixing for Re > 21.0. The streamlines shown for Re=26.4 are representative of those studied in the range of Re > 21.0. Here, we see extensive vortical motion; the streamlines fill much more of the chamber. This apparently chaotic motion, providing distortions and elongations of material interfaces, is responsible for the effective mixing seen at these low Re values.

We demonstrate next suspension mixing of large particles by using fluorescent 10 μm polystyrene beads (Bangs Laboratories, Inc.) in a similar but significantly smaller 3D vortex micromixer (inlet hydraulic diameter of 0.20 mm, chamber diameter of 1.00 mm, and outlet hydraulic diameter of 0.21 mm). We wanted to ensure that mixing improvements are possible even with smaller channels. Beads were flowed into one inlet channel with nonfluorescent aqueous solution in the other. Ideal mixing would result in redistribution of beads such that each outlet channel has the same number of beads and hence fluorescence intensity. We compare the fluorescence intensity distribution in the collection channels at various Re numbers in Fig. 4, and we see again a significant improvement compared to the 2D square-wave design. Surprisingly, the mixing index for the 3D vortex with suspended beads is even better at low Re numbers than the mixing of dissimilar solutions using the larger device (Fig. 2). Further investigations are needed to understand the 3D mixing dynamics of these larger particles as well as the new aspect ratios introduced in this device.

From the experimental data (Figs. 2 and 4), the mixing index of the vortex micromixer is significantly better than the square-wave mixer at all Re numbers tested. The geometrically simple design complemented by ease in fabrication of the low cost and industry-accepted plastic substrate material provides for high-density-layout potential; this would enable the rapid processing of different chemical reactions in parallel arrays on a small chip area [Fig. 4(c)]. Such mixing is critical for applications in—among others—point-of-care diagnostic chips, where the rapid and homogenous mixing of reagents and specimens in small volumes is critical.
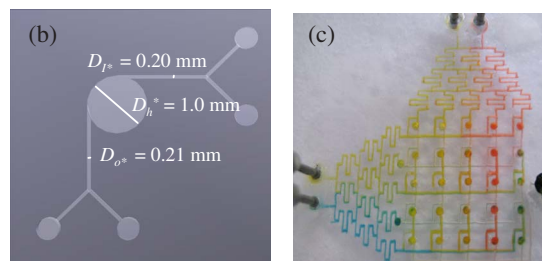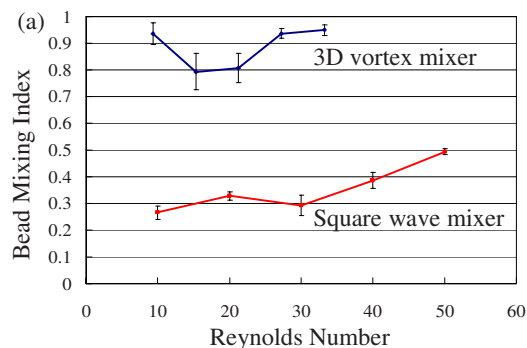
FIG. 4. (Color online) (a) Graph of bead redistribution. of 10 μm diameter. Beads were flown in one inlet channel and solution in the other. Equal distribution of beads in the two outlet channels is quantified as perfect mixing (bead mixing index=1). (b) Smaller 3D vortex mixer used for this study. (c) 5×5 array of micromixers integrated into a microfluidic chip with gradient generators.

[1] H. A. Stone, A. D. Stroock, and A. Ajdari, Annu. Rev. Fluid Mech. **36**, 381 (2004).
[2] P. Yager, T. Edwards, E. Fu, K. Helton, K. Nelson, M. R. Tam, and B. H. Weigl, Nature (London) **442**, 412 (2006).
[3] R. A. Vijayendran, K. M. Motsegood, D. J. Beebe, and D. E. Leckband, Langmuir **19**, 1824 (2003).
[4] B. J. Burke and F. E. Regnier, Anal. Chem. **75**, 1786 (2003).
[5] N. T. Nguyen and Z. Wu, J. Micromech. Microeng. **15**, R1 (2005).
[6] H. M. Xia, S. Y. M. Wan, C. Shu, and Y. T. Chew, Lab Chip **5**, 748 (2005).
[7] J. Aubin, D. F. Fletcher, and C. Xuereb, Chem. Eng. Technol. **26**, 1262 (2003).
[8] J. M. Ottino and S. Wiggins, Science **305**, 485 (2004).
[9] C. J. Campbell and B. A. Grzybowski, Philos. Trans. R. Soc. London, Ser. A **362**, 1069 (2004).
[10] H. Oddy, J. G. Santiago, and J. C. Mikkelsen, Anal. Chem. **73**, 5822 (2001).
[11] A. P. Sudarsan and V. M. Ugaz, Proc. Natl. Acad. Sci. U.S.A. **103**, 7228 (2006).
[12] A. N. Hellman, K. R. Rau, H. H. Yoon, S. Bae, J. F. Palmer, K. S. Phillips, N. L. Allbritton, and V. Venugopalan, Anal. Chem. **79**, 4484 (2007).
[13] X. Niu, L. Liu, W. Wen, and P. Sheng, Appl. Phys. Lett. **88**, 153508 (2006).
[14] K. S. Ryu, K. Shaikh, E. Goluch, Z. Fan, and C. Liu, Lab Chip **4**, 608 (2004).
[15] R. H. Liu, J. Yang, M. Z. Pindera, M. Athavale, and P. Grodzinski, Lab Chip **2**, 151 (2002).
[16] R. H. Liu, M. A. Stremler, K. V. Sharp, M. G. Olson, J. G. Santiago, R. J. Adrian, H. Aref, and D. J. Beebe, J. Microelectromech. Syst. **9**, 190 (2000).
[17] M. A. Stremler, F. R. Haselton, and H. Aref, Philos. Trans. R. Soc. London, Ser. A **362**, 1019 (2004).
[18] A. D. Stroock, S. K. W. Dertinger, A. Ajdari, I. Mezic, H. A. Stone, and G. M. Whitesides, Science **295**, 647 (2002).
[19] C. H. Lin, C. H. Tsai, and L. M. Fu, J. Micromech. Microeng. **15**, 935 (2005).
[20] C. S. Chen, D. N. Breslauer, J. I. Luna, A. Grimes, W. C. Chin, L. P. Lee, and M. Khine, Lab Chip **8**, 622 (2008).
[21] A. Grimes, D. N. Breslauer, M. Long, J. Pegan, L. P. Lee, and M. Khine, Lab Chip **8**, 170 (2008).
[22] P. F. Fischer, J. Comput. Phys. **133**, 84 (1997).